



Flexible Assemblies of Electrocapacitive Volume Tomographic Sensors for Gauging Fuel of Spacecraft

Seung Ho Yang*

LG Display America, Inc., San Jose, California 95131

and

Yong Sik Kim,[†] Nicholas G. Dagalakis,[‡] and Yicheng Wang[§]

National Institute of Standards and Technology, Gaithersburg, Maryland 20899

<https://doi.org/10.2514/1.A34747>

Gauging propellant fuel of spacecraft in outer space has been an issue, because their liquid fuels tend to float, slosh, adhere to the tank walls, and form bubbles under low-gravity conditions. For this reason, conventional fuel gauging techniques may not be an accurate way of gauging the fuel in space. In this paper, we report a flexible monolithic printed assembly of electrocapacitive volume tomography sensors, which can reconstruct the three-dimensional shape of the propellant fuel and promise to overcome the deficiencies of conventional fuel-gauging techniques. A commercial printer was used to transfer the patterns of the electrocapacitive volume tomography sensors and electric connections onto a flexible laminated copper. Feasibility of the three-dimensional volumetric reconstruction on water and a heat-transfer fluid showed that the National Institute of Standards and Technology's flexible electrocapacitive volume tomography sensor system could successfully sense the changes in electrocapacitance due to the presence of these liquids. Based on those measured electrocapacitive volume tomography data, the three-dimensional shape of the fluid was reconstructed and matched with the real one used during laboratory testing.

I. Introduction

GAUGING a spacecraft's fuel quantity is essential for not only managing the vehicle but also for confirming its safety. Approximately 75–90% of a spacecraft's propellant fuel is spent for the desired space orbit-insertion, with the remaining 10–25% for station life keeping [1]. A relatively large uncertainty in the remaining amount of propellant is caused by the liquid apogee motors, which consume a large quantity of propellant for orbit insertion. This uncertainty is important at the end of life (EOL) of the spacecraft for economic reasons [2] and because it could put in danger the lives of its astronauts.

Many combinations of spacecraft propellants and oxidizers have been tested. Commonly used propellants are liquid hydrogen and liquid oxygen, kerosene and liquid oxygen, alcohol and liquid oxygen, gasoline and liquid oxygen, carbon monoxide and liquid oxygen, hydrazine and nitrogen oxides, and hydrazine and beds of catalyst materials [3–5]. Under zero-gravity conditions the spacecraft propellants will adhere to the inner surface of tank walls, constrained by surface tensions and capillary effects [4,6]. Various spacecraft fuel tank liquid free spaces form complex three-dimensional geometries, making the measurement of the remaining propellant a challenging problem.

Several techniques have been developed for the measurement of the onboard amount of a spacecraft's propellant fuel. Some have been tested in space and others have only been tested on the ground. These techniques include the bookkeeping, gas law, thermal gauging method, propellant gauging system, ultrasonic, and capacitive. Following is a brief description of these techniques:

1) The bookkeeping method (BKM) technique requires the integration of the fuel flow rate through the spacecraft thrusters, based on their feed pressure, temperature, and thruster geometry. This technique

is highly accurate at the beginning of the spacecraft mission, when the tank is full, but its accuracy deteriorates with time as fuel is used for spacecraft maneuvering when the tank is depleting as flow measurement errors accumulate [7].

2) The pressure–volume–temperature gas law technique computes the fuel-tank ullage volume based on the initially loaded pressurant gas, usually helium, and the change of pressure and temperature because of fuel use. The EOL fuel volume estimation error of this technique is worse than BKM due to the initial loading condition errors, fuel tank elasticity, heat transfer effects, etc. [8].

3) The propellant gauging system (PGS) technique and the thermal gauging method (TGM) are extensions of the gas law technique [9–12]. They are based on the concept of measuring the thermal capacitance of a fuel tank filled with liquid fuel and a pressurizing gas by using the thermal response of the propellant tank to heating. These techniques have similar error sources as the gas law technique [1,8], but become superior to BKM at EOL.

4) Lal and Raghunandan [13] describe an ingenious technique of an ultrasonic sensor-based spacecraft fuel gauge. The proposed technique uses a titanium alloy cone inside a spherical fuel tank that would collect the fuel at the cone's vertex, which leads to the thruster. Under zero gravity, the greatest forces on the fuel come from surface tension. So, once the fuel has coalesced to form a large mass, it migrates toward the converging end of the cone to minimize its surface area. By bouncing an ultrasound beam off of the surface of the liquid inside the cone and measuring its return time, it is possible to estimate the amount of fuel in the tank. This technique should get more accurate at the EOL as the tank empties. Alternative designs of ultrasonic fuel gauging sensors are reported in [14,15].

5) Hufenbach et al. [16] describes a spin stabilized satellite capacitive sensor, mounted inside a spacecraft fuel propellant tank, for fuel gauging. The sensor uses a coaxial field capacitor to measure the actual filling height of the remaining fuel liquids. An EOL accuracy of $\pm 0.01\%$ is claimed, but no direct comparison with other gauging techniques is possible because it has primarily been developed for a spinning spacecraft.

In this paper, we describe a tomographic instrument that has the ability to reconstruct the three-dimensional (3-D) shape of the propellant fuel and promises to overcome the deficiencies of the previously described techniques. Tomography is a technique that may create an image of the internal structure of an object, without causing damage [17,18]. The word *tomography* comes from the Greek words *tomos*, which means *a section*, and *graphi*, which means *the writing of*

Received 31 January 2020; revision received 13 August 2020; accepted for publication 14 August 2020; published online 9 November 2020. This material is declared a work of the U.S. Government and is not subject to copyright protection in the United States. All requests for copying and permission to reprint should be submitted to CCC at www.copyright.com; employ the eISSN 1533-6794 to initiate your request. See also AIAA Rights and Permissions www.aiaa.org/randp.

*Director, Open Innovation Part, 2540 North First Street.

[†]Research Engineer, Intelligent System Division, Engineering Laboratory, 100 Bureau Dr.

[‡]Senior Research Engineer, Intelligent System Division, Engineering Laboratory, 100 Bureau Dr.

[§]Research Physicist, Quantum Measurement Division, Physical Measurement Laboratory, 100 Bureau Dr.

something. Three-dimensional volume tomography has been invented and may be used to solve the previously mentioned issues with the measurement of the onboard amount of a spacecraft's propellant fuel. Magnetic resonance imaging (MRI), positron emission tomography (PET), x-ray tomography, γ -ray tomography, and electromagnetic tomography are examples of the 3-D tomographic techniques. Those tomography techniques have different sensing mechanisms and are mainly applied to medical diagnosis, clinical oncology, computed tomography of the human body, and food processing [19,20]. The electrocapacitance volume tomography (ECVT) is a recently developed technology. In ECVT, an array of capacitance sensors is used for the imaging of the 3-D shape of the internal objects in a container, a pipe, etc. The ECVT can reconstruct the 3-D images of the internal objects based on the measured capacitance signals [21,22].

Recently, attention has been given to flexible sensors [23]. Artificial electronic skins, wearable consumer electronics, soft robotics, and real-time health monitoring sensors are emerging examples of the application of flexible sensors. They are lightweight, flexible, and wearable physical sensors with distinctive functionalities. These flexible sensors can conform and attach to rounded bodies and containers so that they may maximize their sensing capability. Sensor strips of the ECVTs can be made from copper plates manually. This is simple and straightforward, but it is not easy to build the exact same shape of the sensor strips and align them along the neighboring elements with the same gaps. In this paper, we report a monolithic printed assembly of electrocapacitive volume tomography sensors, which can reconstruct the three-dimensional shape of the propellant fuel and promise to overcome the deficiencies of conventional fuel-gauging techniques.

One alternative to sensor strips of the ECVTs made from copper plates manually is soft lithography [24–27], which is a fabrication technique using commercial printers and a paper-thin laminated copper sheet. The printer can transfer lithographic patterns onto the paper-thin laminated copper sheet. Wax-coated solid inks are printed onto the laminated sheet, and form the patterns of the ECVT sensors and their electric connections. The printed flexible strip is then etched, and the printed wax-containing inks are removed to produce the flexible ECVT monolithic sensor strips. These flexible ECVT sensor strips are applied to rounded vessels to measure the changes in the electric capacitance related to the presence of a liquid. For evaluation of the approach, a liquid that had almost the same dielectric constant as spacecraft fuels was used. Results showed clear variations in the measured electric capacitance with the presence of the liquid. The reconstructed 3-D image showed a good match with the real shapes of the liquids.

II. ECVT Sensor Design and Fabrication

A. Materials

For fabricating the ECVT sensor strips, Dupont Pyralux laminated sheets are used. These sheets have a copper layer of 9 μm in thickness and a Kapton layer of 25 μm in thickness. Xerox solid inks were used to transfer the predetermined patterns of the ECVT sensors and the electric connections. These solid inks consist of wax-coated ink particles with a mixture of four different color toners (Cyan, Magenta, Yellow, Black), making it easy to detect the quality of lithographic pattern transfer. To etch the copper, ferric chloride was used. Acetone was used to remove the wax-ink from the lithographic pattern. Isopropyl alcohol and double-filtered water were used for the cleaning.

B. Sensor Design and Optimization

A commercial solid-ink laser printer (Xerox Phaser 6360N[†]) was used for the lithographic pattern transfer. Semisolid wax-coated solid ink particles were melted and transferred from the drum onto a heated laminated sheet. The design of the ECVT sensor strips was prepared by either computer-aided design software or other drawing tools for

[†]Certain trade names and company products are mentioned in the text or identified in an illustration to adequately specify the experimental procedure and equipment used. In no case does such an identification imply recommendation or endorsement by the National Institute of Standards and Technology, nor does it imply that the products are necessarily the best available for the purpose.

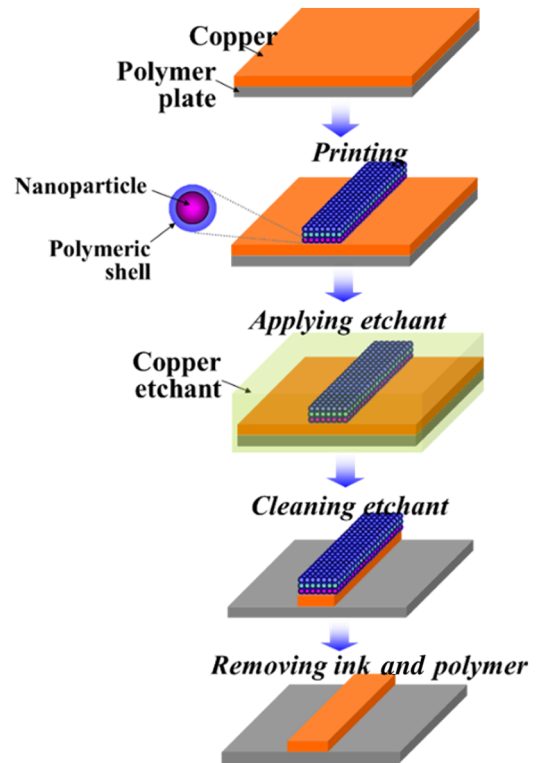


Fig. 1 Schematic illustration of the ECVT sensor fabrication process.

vector drawing. Three different solid inks, cyan, magenta, and yellow, are overwritten onto the same spot to form the black color, and these become the lithographic patterns of sensors and electric connections. The printed laminates are then etched with ferric chloride in a clean chamber. After the etching, the etching residues are cleaned with isopropyl alcohol, double-filtered distilled water, and nitrogen blowing. The strip is immersed in acetone to remove the wax and inks used for the etch-protection layer. Then, the strip is cleaned with isopropyl alcohol, double-filtered distilled water, and nitrogen blowing. The schematic fabrication process of the ECVT sensor strip is illustrated in Fig. 1.

C. Sensor Fabrication Process

If the dielectric constant of the liquid ϵ_L in the vessel is much greater than the dielectric constant of the air ϵ_{air} in the vessel, then the ECVT data generated by the liquid in the vessel dominates the final fuel images generated by the instrument. This is the case when the liquid is water, which has a dielectric constant about 80 times larger than that of air. For this reason, it would be easy to detect the 3-D shape of the liquid inside the vessel and no optimization on electrode design would be needed.

However, if the dielectric constant ϵ_L of the liquid in the vessel is not much greater than ϵ_{air} , then the measured data can be disturbed by other effects like the variation in fabrication of the ECVT sensor strip and the vessel. Actually, the ϵ_L of the National Aeronautics and Space Administration's (NASA's) sample liquid is 1.73, which is not significantly larger than that of air ($\epsilon_{\text{air}} = 1.00$). Therefore, the optimization of the sensor design to maximize data sensitivity is one of the keys to successfully measuring the 3-D shape of the liquid in the vessel.

The optimum design of the ECVT sensors is schematically illustrated in Fig. 2. The design of the sensors started with simple parallel electrode plates, which are shown in Fig. 2a. Because of the sensor design, the electric field measured through the gap formed by the edges between the electrodes dominates the measured data. Tests also showed that the measured data contain the variation of the electric field outside of the vessel, shown in Fig. 2a. Adding an electric shielding layer (Fig. 2b) eliminates the influence from the electric field outside of the vessel. Still, the electric field formed by the edges between the gap is present. Figure 2c shows the final design of the electrodes. The addition of extra strips from the electric shielding layer removed the influence of

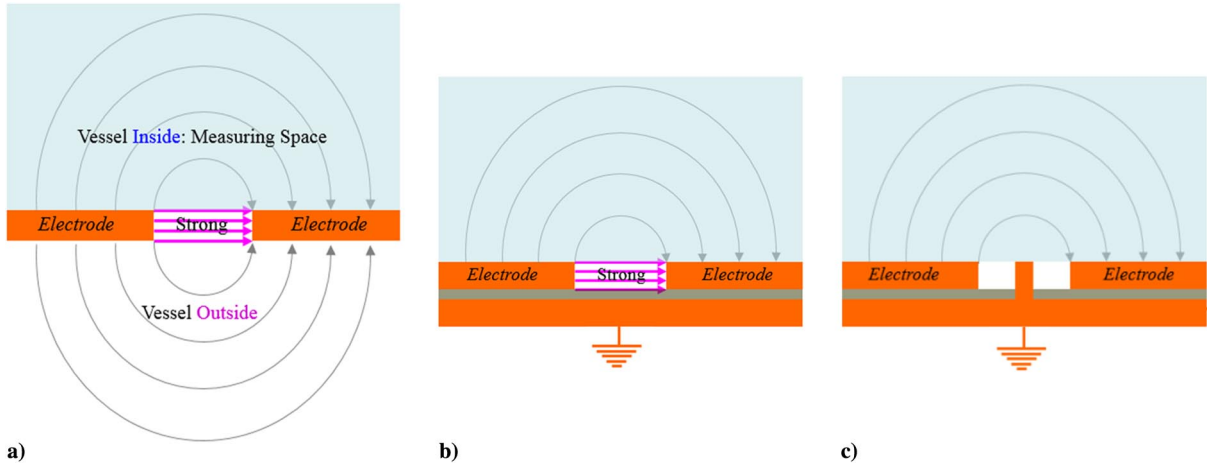


Fig. 2 Schematic illustration of the optimized design of the ECVT sensor.

the electric field between the sensor electrodes, so that only the variation of the electric field in the vessel is measured.

III. Feasibility Studies of the Proposed ECVT Sensors

A. Fabrication and Testing of a Single-Strip ECVT

Single-strip ECVT sensors are fabricated with the process described in Sec. II. One example of the fabricated sensor strip is shown in Fig. 3. The front side (Fig. 3a) has four sensors and electric line connections. One of these lines is connected to the electric shielding located between every two sensors, as described in Sec. II.C, to cancel out the direct electric field between the two sensors. Figure 3b shows the back side of the fabricated sensor plate. This shielding layer

and the front-side layers are electrically separated by a 25 μm Kapton layer. The front shielding layer is shown in Fig. 3c. The schematic illustration on the vertical cross section of the sensor strip is illustrated in Fig. 3d.

These sensor strips are then covered with a waterproof coating and are enclosed in a plastic jar, as shown in Fig. 4. The electrocapacitances between each pair of the sensors are measured with an Andeen-Hagerling capacitance bridge (model AH2700A), which is also shown in Fig. 4. The configuration of the electrodes is shown in Fig. 4b. A feasibility test capacitance measurement with the jar setup (Fig. 4) was carried out under different water-level heights. Figure 5 shows that, for all of the electrode pair combinations, capacitance measurements showed almost a linear increase with respect to the water height.

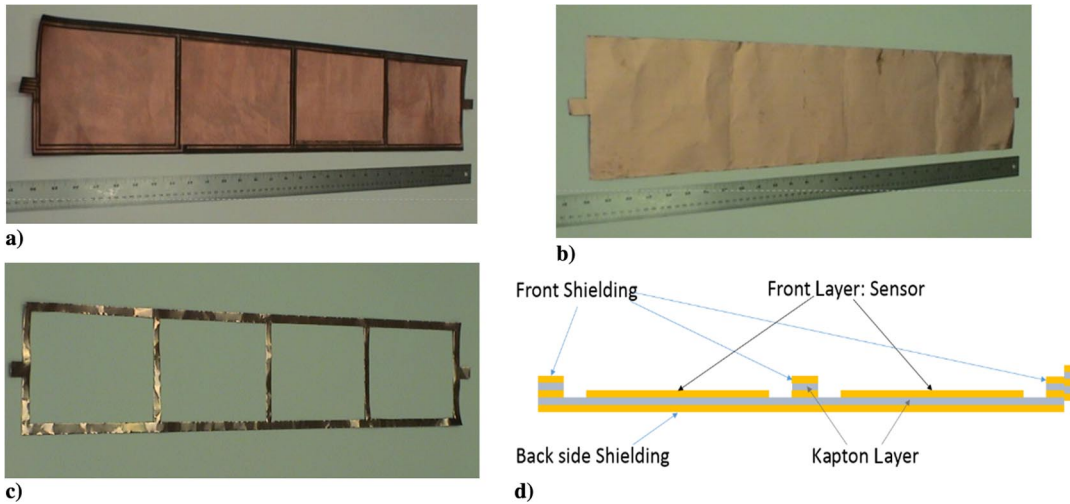


Fig. 3 Example of the fabricated sensor strip: a) front side, b) back side, c) front shielding, and d) schematic illustration of the cross section of the sensing strip.

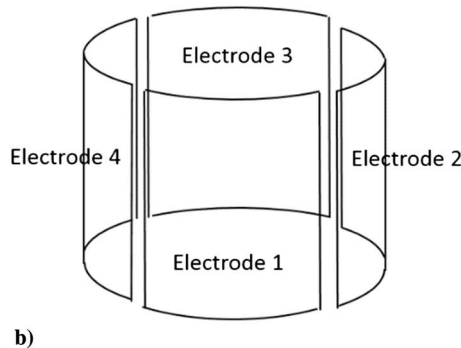
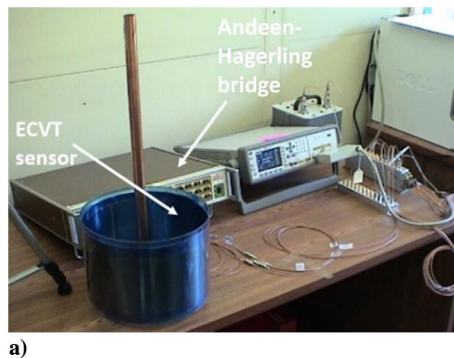


Fig. 4 Experimental setup and sensor electrode configuration of one-strip ECVT sensor: a) experimental setup, and b) electrode configuration.

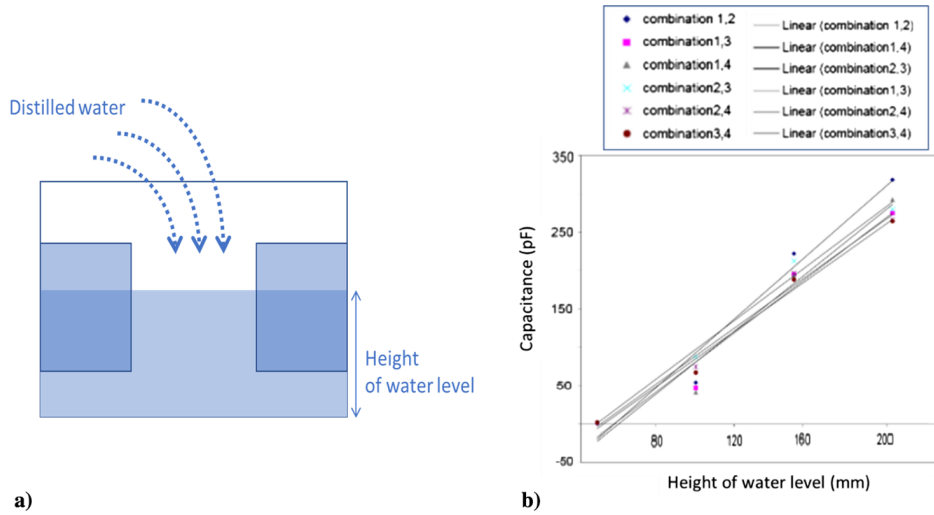


Fig. 5 Effect of water level on measured capacitance data for all electrode pairs.

B. Fabrication and Testing of a Three-Strip ECVT Sensor

The three-strip ECVT sensor was installed on the wall of an egg-shaped container vessel. For this, the container vessel shown in Fig. 6a is suspended with four springs to a frame and wrapped with the ECVT sensor. This ECVT sensor consists of three rows, one of which has four electrodes in a zigzag pattern, as shown at the right in Fig. 6b. The cross-sectional view of the vessel is shown at the left in Fig. 6b. The shape of the vessel is designed to simulate a smaller version of a

NASA spacecraft’s fuel tank. Three ECVT sensor rows are installed on the internal surface of the vessel, and the surface of the vessel is electrically grounded.

To run feasibility tests, an additional cylinder whose internal surface is connected to the ground is added onto the egg-shaped container vessel to minimize the influence of any laboratory external disturbances. The schematic illustration of the design is given in Fig. 7. Different sized rubber balls, which have diameters of 8.5, 10.5,

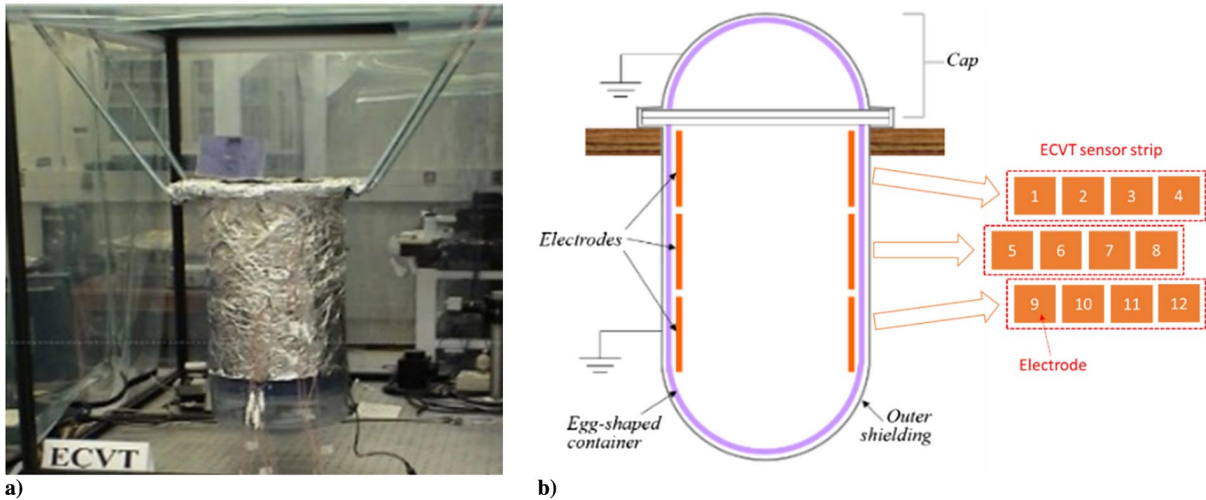


Fig. 6 Experimental ECVT setup at NIST: a) a photograph of the setup, and b) the configuration of the electrodes.

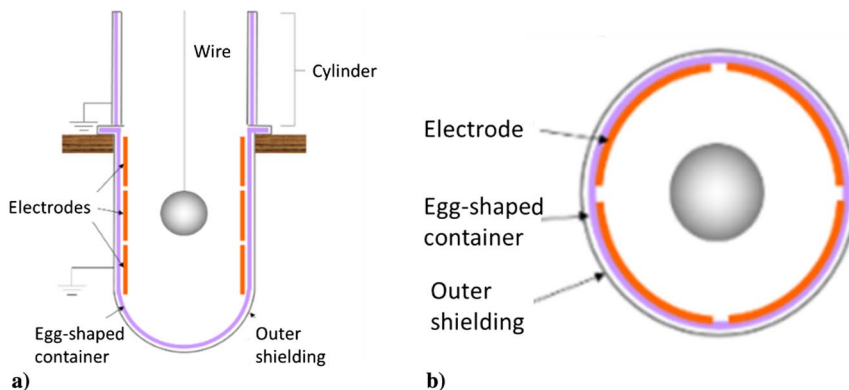


Fig. 7 Schematic illustrations of the ECVT container with multisensor strips, and rubber balls suspended in its interior (ball diameters: 8.5, 10.5, and 12 cm).

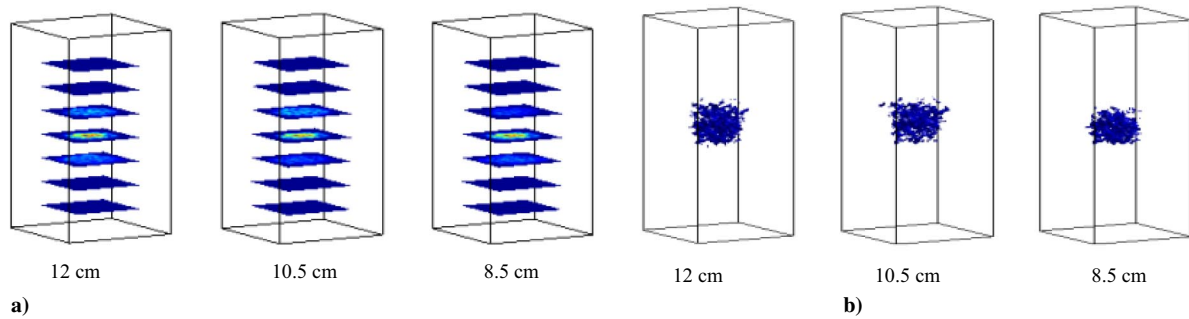


Fig. 8 Reconstructed 2D and 3D shapes for the rubber balls with diameters of 8.5 cm, 10.5 cm, and 12 cm.

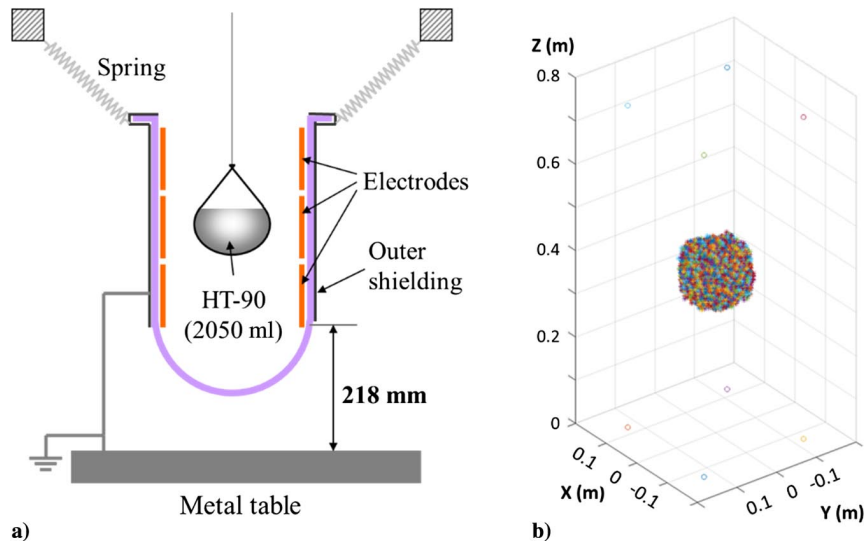


Fig. 9 Schematic diagram for testing HT-90 in a balloon and its reconstructed 3-D shape.

and 12 cm, respectively, are suspended in air within the container for testing (Fig. 7).

The measured ECVT data were analyzed and used to reconstruct the volumetric dielectric profile given by NASA and a CTech Laboratories company [28]. As described in a patent [29], the reconstruction method relied on a neural-network optimization technique, using the soft-field nature of the so-called fringing effect of the electric field that distributes in three-dimensional space. The fringing effect contains valuable information that can be extracted using a soft-computing algorithm for imaging purposes.

Figure 8a shows the reconstructed shapes of the rubber balls suspended in air, projected on equally spaced two-dimensional (2-D) layers for the 8.5, 10.5, and 12 cm rubber balls. The reconstructed 3-D images of those rubber balls are shown in Fig. 8b. These reconstructed data show that the multistrip ECVT sensors work. The ECVT data with a Golden HT-90 heat transfer fluid in a plastic balloon, suspended in air, which has similar dielectric constants with the fuel of the NASA spacecraft, was tested to see if the National Institute of Standards and Technology's (NIST's) multilayer ECVT strips could measure and reconstruct its 3-D shape. The schematic illustration of the balloon is given in Fig. 9a. Its reconstructed 3-D shape is given in Fig. 9b. The diameter of the balloon is 157.6 mm and the corresponding measurement ranges from 148.1 to 153.2 mm, indicating that the error of the reconstructed result is less than 6% of its original diameter. In the future, plans will be to perform more testing and explore with NASA other image-reconstruction techniques, such as the recently proposed iterative nonlinear Tikhonov regularized algorithm [30], to further improve the ECVT method.

IV. Conclusions

The design of the sensor strips is optimized to maximize the sensitivity of the measured ECVT data to the vessel target material. A single-strip ECVT sensor could successfully measure the water

levels. A multilayer-strip ECVT sensor could measure and reconstruct the shapes of rubber balls located in the vessels because of the increased number of electro plates. NIST's multilayer ECVT strips were installed in the egg-shaped vessels, which are smaller versions of the fuel tank of NASA's spacecraft. It has been demonstrated because of the increased number of electro plates that it could reconstruct the 3-D shape of HT-90 balloons in the test vessel.

Acknowledgments

This work was supported in part by the Innovative Partnerships Program of NASA for work in "Cryogenic Fuel Gauge for Zero Gravity Environments Using Capacitance Tomography." The authors would like to thank Manohar Deshpande and Lawrence M. Hilliard, of the NASA Goddard Space Flight Center, for their valuable advice and support. This research was performed in part at the National Institute of Standards and Technology Center for Nanoscale Science and Technology Nano Fabrication Clean Room.

References

- [1] Chobotov, M. V., and Purohit, G. P., "Low-Gravity Propellant Gauging System for Accurate Predictions of Spacecraft End-of-Life," *Journal of Spacecraft and Rockets*, Vol. 30, No. 1, Jan.–Feb. 1993, pp. 92–101. <https://doi.org/10.2514/3.25475>
- [2] Ambrose, J., Yendler, B., and Collicott, S. H., "Modeling to Evaluate a Spacecraft Propellant Gauging System," *Journal of Spacecraft and Rockets*, Vol. 37, No. 6, Nov.–Dec. 2000, pp. 833–835. <https://doi.org/10.2514/2.3642>
- [3] Mishra, D. P., "Fundamentals of Rocket Propulsion," CRC Press, 2017.
- [4] Gibbon, D. M., and Bellerby, J. M., "Simulation of Conditions Inside a Spacecraft Bipropellant Tank," *AIAA/ASME/SAE/ASEE 24th Joint Propulsion Conference*, AIAA Paper 1988-2923, July 1988. <https://doi.org/10.2514/6.1988-2923>
- [5] "Spacecraft Propulsion," NASA, Washington, D.C., <https://mars.nasa.gov/mro/mission/spacecraft/parts/propulsion/> [retrieved 18 Jan. 2020].

- [6] Phillips, T., "The Strange Way Fluids Slosh on the International Space Station," *NASA Science Newsletter*, https://science.nasa.gov/science-news/science-at-nasa/2015/30jan_slosh [retrieved 18 Jan. 2020].
- [7] Yendler, B., "Review of Propellant Gauging Methods," *44th AIAA Aerospace Sciences Meeting and Exhibit*, AIAA Paper 2006-0939, Jan. 2006. <https://doi.org/10.2514/6.2006-939>
- [8] Bergaglio, B., Brandt, R., Caporicci, M., Kaisch, L., and Schoyer, H. F. R., "Recent Experiences in European Liquid Spacecraft Propulsion," *31st Aerospace Sciences Meeting and Exhibit*, AIAA Paper 1993-690, Jan. 1993. <https://doi.org/10.2514/6.1993-690>
- [9] Yip, A., Yendler, B., Martin, T. A., and Collicott, S. H., "Anik E Spacecraft Life Extension," *Space Ops 2004 Conference*, AIAA Paper 2004-0208, 2004. <https://doi.org/10.2514/6.2004-367-208>
- [10] Aparicio, A., and Yendler, B., "Thermal Propellant Gauging at EOL, Telstar 11 Implementation," *SpaceOps2008Conference*, AIAA Paper 2008-3375, 2008. <https://doi.org/10.2514/6.2008-3375>
- [11] Ahmed, M. E., Nemri, O., Yendler, B., and Chernikov, S., "Implementation of Thermal Gauging Method for SpaceBus 3000A (ArabSat 2B)," *SpaceOps Conference*, AIAA Paper 2012-1269441, 2012. <https://doi.org/10.2514/6.2012-1269441>
- [12] Yendler, B., Chernikov, S., Molinsky, J., and Guadagnoli, D., "Comparison of Gauging Methods for Orbital's GEOStar[™]1 Satellites," *SpaceOps Conferences*, AIAA Paper 2014-1810, May 2014. <https://doi.org/10.2514/6.2014-1810>
- [13] Lal, A., and Raghunandan, B. N., "Configuration of Propellant Gauging in Satellites," *Journal of Spacecraft and Rockets*, Vol. 44, No. 1, Jan.–Feb. 2007, pp. 143–146. <https://doi.org/10.2514/1.20709>
- [14] Murolo, F., Bihl, C., Pili, P., Klinc, M., and Brandt, R., "The Ultrasonic Gauging Sensors: Results of an Innovative Spacecraft Propellant Measurement Method," *SpaceOps Conferences*, AIAA Paper 2014-1938, May 2014. <https://doi.org/10.2514/6.2014-1938>
- [15] Bihl, C., Murolo, F., Klinc, M., Achkar, I. M., and Robert, B., "Propellant Gauging Experience with Meteosat Second Generation S/C Fleet," *SpaceOps Conferences*, AIAA Paper 2018-2319, May–June 2018. <https://doi.org/10.2514/6.2018-2319>
- [16] Hufenbach, B., Brandt, R., Andre, G., Voeten, R., van Put, P., Sanders, B., Schwer, A., Delil, A., Mastenbroek, O., and Pauw, A., "Comparative Assessment of Gauging Systems and Description of a Liquid Level Gauging Concept for a Spin Stabilized Spacecraft," *Proceedings Second European Spacecraft Propulsion Conference*, European Space Agency SP-398, Paris, Aug. 1997, pp. 561–570.
- [17] Fan, Z., and Gao, R. X., "Enhancement of Measurement Efficiency for Electrical Capacitance Tomography," *IEEE Transactions on Instrumentation and Measurement*, Vol. 60, No. 5, 2011, pp. 1699–1708. <https://doi.org/10.1109/TIM.2011.2113010>
- [18] Cui, Z., Wang, H., and Yin, W., "Electrical Capacitance Tomography with Differential Sensor," *IEEE Sensors Journal*, Vol. 15, No. 9, Sept. 2015, pp. 5087–5094. <https://doi.org/10.1109/JSEN.2015.2446982>
- [19] Herman, G. T., *Fundamentals of Computerized Tomography: Image Reconstruction from Projection*, 2nd ed., Springer, Berlin, 2009.
- [20] Banhart, J., "Advanced Tomographic Methods in Materials Research and Engineering," *Monographs on the Physics and Chemistry of Materials*, Oxford Univ. Press, New York, 2008.
- [21] Huang, S. M., Plaskowski, A. B., Xie, C. G., and Beck, M. S., "Capacitance-Based Tomographic Flow Imaging System," *Electronics Letters*, Vol. 24, No. 7, March 1988, pp. 418–419. <https://doi.org/10.1049/el:19880283>
- [22] Wang, F., Marashdeh, Q., Fan, L.-S., and Warsito, W., "Electrical Capacitance Volume Tomography: Design and Applications," *Sensors*, Vol. 10, No. 3, Oct. 2010, pp. 1890–1917. <https://doi.org/10.3390/s100301890>
- [23] Bessonov, A. A., and Kirikova, M. N., "Flexible and Printable Sensors," *Nanotechnologies in Russia*, Vol. 10, Nos. 3–4, May 2015, pp. 165–180. <https://doi.org/10.1134/S1995078015020044>
- [24] Xia, Y., and Whitesides, G. M., "Soft Lithography," *Angewandte Chemie International Edition in English*, Vol. 37, No. 5, Dec. 1998, pp. 550–575. [https://doi.org/10.1002/\(SICI\)1521-3773\(19980316\)37:5<550::AID-ANIE550>3.0.CO;2-G](https://doi.org/10.1002/(SICI)1521-3773(19980316)37:5<550::AID-ANIE550>3.0.CO;2-G)
- [25] Xia, Y., and Whitesides, G. M., "Soft Lithography," *Annual Review of Material Science*, Vol. 28, No. 1, 1998, pp. 153–184. <https://doi.org/10.1146/annurev.matsci.28.1.153>
- [26] Quake, S. R., and Scherer, A., "From Micro- to Nanofabrication with Soft Materials," *Science*, Vol. 290, No. 5496, 2000, pp. 1536–1540. <https://doi.org/10.1126/science.290.5496.1536>
- [27] Rogers, J. A., and Nuzzo, R. G., "Recent Progress in Soft Lithography," *Materials Today*, Vol. 8, No. 2, Feb. 2005, pp. 50–56. [https://doi.org/10.1016/S1369-7021\(05\)00702-9](https://doi.org/10.1016/S1369-7021(05)00702-9)
- [28] "Non-Destructive Testing and Material Inspection," CTECH LABS, Powai, Mumbai, India, <http://www.c-techlabs.com/non-destructive-testing-and-material-inspection/> [retrieved July 2019].
- [29] Warsito, W., and Fan, L. S., U.S. Patent PTO 6577700, 2003.
- [30] Xu, F., and Deshpande, M., "Iterative Nonlinear Tikhonov Algorithm with Constraints for Electromagnetic Tomography," *IEEE Journal of Selected Topics in Applied Earth Observations and Remote Sensing*, Vol. 5, No. 3, June 2012, pp. 707–716. <https://doi.org/10.1109/JSTARS.2012.2193117>

D. P. Thunnissen
Associate Editor